Effects of Chain End Structures on Pyrolysis of Poly(L-lactic acid) Containing Tin Atoms

著者	Mori Tomokazu, Nishida Haruo, Shirai Yoshihito, Endo Takeshi
雑誌名	Polymer Degradation and Stability
巻	84
号	2
ページ	243-251
発行年	2004-05-06
URL	http://hdl.handle.net/10228/00006746

doi: info:doi/10.1016/j.polymdegradstab.2003.11.008

Effects of Chain End Structures on Pyrolysis of Poly(L-lactic acid) Containing Tin Atoms

Tomokazu Mori[a,b], Haruo Nishida[a,*], Yoshihito Shirai[c], and Takeshi Endo[a,d]

[a] *Molecular Engineering Institute, Kinki University, 11-6 Kayanomori, Iizuka, Fukuoka 820-8555, Japan*

[b] *Faculty of Computer Science and Systems Engineering, Kyushu Institute of Technology, 680-4 Kawazu, Iizuka, Fukuoka, 820-8502, Japan*

[c] *Graduate School of Life Science and Systems Engineering, Kyushu Institute of Technology, 1-1 Hibikino, Kitakyushu, Fukuoka 808-0196, Japan*

[d] *Faculty of Engineering, Yamagata University, 4-3-6 Jonan, Yonezawa,Yamagata 992-8510, Japan*

*Corresponding author: Haruo Nishida

Molecular Engineering Institute, Kinki University, Fukuoka 820-8555, Japan

Tel / Fax: +81-948-22-5706.

E-mail address: hnishida@mol-eng.fuk.kindai.ac.jp (H. Nishida)

Abstract

Thermal degradation of high molecular weight PLLA containing residual tin atoms was investigated as a means of controlling the reaction for feedstock recycling to L,L-lactide. To clarify the pyrolysis mechanism of the PLLA, three samples with different chain end structures were prepared, namely, as-polymerized PLLA-ap, precipitated-with-methanol PLLA-pr, and purified PLLA-H. From pyrolyzate and kinetic analyses, typical degradation mechanisms of Sn-containing PLLA were clarified. In other words, it was assumed that the pyrolysis of PLLA-ap proceeds through a zero-order weight loss process with the apparent E_a = 80-90 kJ mol^{-1}, and with the occurrence of backbiting and transesterification reactions caused by Sn-alkoxide chain ends. The pyrolysis of PLLA-pr was also assumed to proceed via a zero-order weight loss process with apparent E_a = 120-130 kJ mol^{-1}, with the proposed mechanism being Sn-catalyzed selective lactide elimination caused by Sn-carboxylate chain ends. Both pyrolysis of PLLA-ap and PLLA-pr produced L,L-lactide selectively. These degradation mechanisms and products are in contrast to those of PLLA-H, in which a large amount of diastereoisomers and cyclic oligomers were formed by random degradation. From this study, the complicated PLLA pyrolysis behavior as reported previously could be explained properly.

Keywords: poly(L-lactic acid), poly(L-lactide), PLLA, thermal degradation, pyrolysis, kinetic analysis, feedstock recycling, end structure, kinetic parameter

1. Introduction

Poly(L-lactic acid) {poly(L-lactide), PLLA} is a well-known biodegradable polymer. It has received much interest for its medical, pharmaceutical, and environmental applications [1-3]. Nowadays, because of its many useful properties, such as mechanical strength, transparency, and compostability [4-6], PLLA and its related copolymers are attracting much attention as promising alternatives to the commodity resins [7]. PLLA is generally prepared by the ring-opening polymerization of L,L-lactide [8-11], and the thermal degradation of PLLA results in the recovery of L,L-lactide [12,13]. This chemical property of PLLA makes it a possible candidate as a feedstock recycling plastic. However, the thermal degradation of PLLA is more complex than the simple reaction that gives L,L-lactide. The activation energy, E_a, of degradation has been reported to change irregularly in the range 70-190 kJ mol^{-1} as the degradation progresses. For example, irregular behavior occurs at 110’ 190 kJ mol^{-1} (Kopinke et al. [14]), at 103’ 72’ 97 kJ mol^{-1} (Babanalbandi et al. [15]), and at 95’ 80’ 160 kJ mol^{-1} (Aoyagi et al. [16]). Moreover, many kinds of degradation products have been detected during the pyrolysis of PLLA, especially *meso*-lactide, D,D-lactide, and cyclic oligomers, all of which cause serious problems after the reproduction of PLLA, by diminishing some of its useful properties, such as crystallizability [17-19]. Thus, it is very important to determine the degradation mechanisms of high molecular weight PLLA and to control these mechanisms to selectively produce L,L-lactide for the feedstock recycling.

The factors that influence the thermal degradation of PLLA apart from molecular weight include the presence of moisture, residual and hydrolyzed monomers, oligomers, and residual metals. In particular, the

effect of residual tin compounds is very important, because only tin 2-ethylhexanoate {$Sn(Oct)_2$} has been approved by the FDA as a catalyst [20]. Though many reports have shown the accelerating effect of {$Sn(Oct)_2$} on PLLA pyrolysis, the degradation mechanisms have been discussed in only a few reports. Södergård and Näsman demonstrated that, based on the melt viscosity changes, the thermal degradation of PLLA containing 690 ppm of Sn proceeded through a random main-chain scission with apparent activation energy E_a=119.4 kJ mol^{-1} [21]. Kopinke et al. studied the weight loss behavior on the pyrolysis of PLLA containing 250 ppm of Sn [14]. They found two well-resolved peaks in the DTG profile. From pyrolyzates and degradation kinetics analyses, the low and high temperature decomposition reactions were evaluated as a Sn-catalyzed depolymerization starting from hydroxyl chain ends with E_a=110 kJ mol^{-1} and random transesterification reactions to produce cyclic oligomers, respectively. A first-order kinetic treatment was used for the evaluation of the low temperature decomposition reaction. Wachsen et al. compared the thermal degradation behavior between the two types of PLLAs (Sn content: 15 and 145 ppm) in sealed ampoules, and E_a values: 120 and 92 kJ mol^{-1} for the two samples, respectively, were calculated based on the random degradation/recombination equilibrium equations [22].

As mentioned in many previous reports, the accelerating effect of Sn atoms on thermal degradation of PLLA is clear, however it has not yet clearly been established whether the main degradation mechanism is a 1st-order reaction or a random reaction. In our previous report [23], to analyze accurately the effect of the Sn atom on pyrolysis, PLLA samples with various amounts of Sn content (20-607 ppm) were prepared and the thermal degradation kinetics and mechanisms were investigated. It was found that the pyrolysis of

PLLA samples with Sn content of < 20 ppm proceeded mainly through a random degradation (E_a = 180-190 kJ mol^{-1}) and the contrastive samples with Sn content of > 485 ppm were evaluated as proceeding via a zero-order weight loss process (E_a = 120-130 kJ mol^{-1}) as a main route. Further, it was clarified that in all samples the degradation kinetics and mechanisms gradually changed with temperature. For example, in the pyrolysis of PLLA-Sn (607 ppm) there was a change from a random degradation in the initial stage to the zero-order weight loss behavior in the main stage. The previously reported complicated PLLA pyrolysis behavior is explainable in part by such results. However, sometimes a degradation process with E_a value less than 100 kJ mol^{-1} was encountered, which though reported by Wachsen et al. [22] and Babanalbandi et al., [15] has not yet been clarified.

In this work, our attention was directed to the effect of PLLA-Sn end structure on the pyrolysis. Kricheldorf et al. reported that the polymerization of L,L-lactide proceeds most likely via the relatively reactive Sn-alkoxide group [24]. Further, they pointed out that these Sn-alkoxide groups will be transformed into -CH-OH end-groups via alcoholysis or hydrolysis. This is a very important point to note when considering the chemical recycling of PLLA, because the products are inevitably exposed to water and protic additives in processing, as well as moisture from the environment etc. Thus, in this study, as-polymerized PLLA and precipitated PLLA with methanol were prepared, whilst there still remained plenty of Sn compounds in the form of catalyst residue. The dynamic thermal degradation and volatile products analyses of the samples were carried out in comparison with those of a metal-free PLLA. Finally, the characteristic degradation mechanisms of the samples were discussed.

2. Experimental

2.1. Materials

Monomer, L,L-lactide, was obtained from Shimadzu Co. Ltd. It was composed of 99.4 % L,L-lactide and 0.6 % *meso*-lactide according to a gas chromatography (GC) measurement. This monomer was recrystallized three times from dry toluene and then once from dry ethyl acetate. After the purification, *meso*-lactide was not detectable by GC. The vacuum dried L,L-lactide was stored in an N_2 atmosphere. A catalyst, tin 2-ethylhexanoate {$Sn(Oct)_2$} was obtained from Wako Pure Chemical Industries, Ltd. and distilled under reduced pressure before use. Ammonia solution (25 %) and hydrochloric acid (1**M**) specifically produced for the atomic absorption spectrophotometry were purchased from Wako Pure Chemical Industries, Ltd. and used as received.

2.2. Preparation of PLLA samples

PLLA was synthesized by the ring-opening polymerization of L,L-lactide catalyzed by $Sn(Oct)_2$ in bulk. A molar ratio [catalyst]/[monomer] = 1/1000 in feed and a multi-temperature process (150 ℃ / 0.5 h + 130 ℃ / 5 h + 110 ℃ / 13 h + 90 ℃ / 12 h) were employed in the polymerization. Purified L,L-lactide 5.081 g (35.3 mmol) was added into a reaction tube in a glove box under N_2 atmosphere. Then, $Sn(Oct)_2$ 12.55 μL (0.0157 g, 34.4 μmol) was added by using a micro syringe. The reaction tube was connected to a vacuum line and the toluene was allowed to evaporate for 48 h *in vacuo*. After sealing in a flame, the tube

was immersed into an oil bath. After the polymerization, as-polymerized PLLA (PLLA-ap) was obtained as a white solid with a ~100 % yield based on a ^{1}H-NMR analysis. PLLA-ap 3.825 g was dissolved in chloroform 150 mL and precipitated with 10-fold of methanol to prepare precipitated PLLA (PLLA-pr) 3.552 g with a 92.87 % yield. Residual Sn compounds in PLLA-pr were extracted from a solution of PLLA-pr (2.4373 g) / chloroform (150 mL) three times with 300 mL of 1**M** HCl aqueous solution, then washed with distilled water until the aqueous phase became totally neutral. Finally, the polymer was precipitated with methanol to prepare the purified PLLA (PLLA-H) with a 46.10 % yield.

The molecular weight and Sn content of the three PLLA samples are listed in Table 1. For preparing sample films, each chloroform solution of the corresponding sample (0.3 g in 20 mL $CHCl_3$) was cast on a glass Petri dish surface. After the evaporation of the solvent, the formed film was washed by methanol and then vacuum dried.

[**Table 1.** PLLA samples]

2.3. Dynamic pyrolysis

Thermogravimetric analysis (TG/DTA) was conducted on a Seiko Instruments Inc. EXSTAR 6200 TG system in aluminum pans under a constant nitrogen flow (100 mL min^{-1}) using about 8 mg of the PLLA film sample. For each sample, prescribed heating rates of 1, 3, 5, 7, and 9 K min^{-1} were applied from room temperature to 400°C. The pyrolysis data were collected at regular intervals (about 20 times K^{-1}) by an EXSTAR 6000 data platform, and recorded into an analytical computer system.

2.4. Measurements

^{1}H-NMR spectra were recorded on a Varian INOVA400 NMR spectrometer operating at 400 MHz for proton investigation in chloroform-*d* solution with tetramethylsilane as the internal standard.

The gas chromatography (GC) measurements were recorded on a Shimadzu GC-9A gas chromatograph with a Varian cyclodextrine-² -236M-19 capillary column (0.25 mm × 50 m) using helium as the carrier gas. The column and injector were set isothermally at 150 and 220 ºC, respectively. The sample (3 mg) was dissolved in acetone (1 mL) and a 1 µL aliquot of the solution was injected. The peaks for *meso*-, L,L-, and D,D-lactides were identified by comparison with pure substance peaks.

Gel permeation chromatography (GPC) was measured on a TOSOH HLC-8220 GPC system at 40ºC using TOSOH TSKgel Super HM-H column and chloroform eluent (0.6 mL min^{-1}). Low polydispersity polystyrene standards with M_n from 5.0×10^2 to 1.11×10^6 were used for calibration. The sample (12 mg) was dissolved in chloroform (2 mL) and the solution was filtered through a membrane filter having a 0.5 µm pore size.

The Sn content in the PLLA samples was measured with a Shimadzu AA-6500F atomic absorption flame emission spectrophotometer (AA). The sample was degraded by a 25 % ammonia solution, dissolved in 1**M**-hydrochloric acid, and then measured by AA.

Pyrolysis-gas chromatograph/mass spectra (Py-GC/MS) were recorded on a Frontier Lab double-shot pyrolyzer PY-2020D with a Frontier Lab SS-1010E selective sampler and a Shimadzu GCMS-QP5050

chromatograph/mass spectrometer. High purity helium was used as carrier gas at 50 mL min^{-1}. The volatile products were analyzed with an Ultra Alloy^{+}-5 capillary column (30 m × 0.25 mm i.d.; film thickness, 0.25 μm). A PLLA sample was put in the pyrolyzer and heated from 60 ºC to a prescribed temperature at a heating rate of 10 ºC min^{-1}. The volatile pyrolysis products were introduced into the GC through the selective sampler. The temperature of column oven was first set at 40°C. After the pyrolysis process had finished, the column was heated according to the following program: 40 ºC for 1 min; 40-120 ºC at 5 ºC min^{-1}; 120-320 ºC at 20 ºC min^{-1}; 320 °C for 13 min. Mass spectrum measurements were recorded 2 times s^{-1} during this period.

3. Results and Discussion

3.1. Preparation of PLLA samples

To clarify the effect of PLLA-Sn end structure on the thermal degradation of PLLA, three samples were prepared (Table 1). Original PLLA was synthesized through the ring-opening polymerization, using tin 2-ethylhexanoate {$Sn(Oct)_2$} as a catalyst. The polymerization proceeded completely with ~100 % yield to form “as-polymerized PLLA” (PLLA-ap), a white solid polymer, containing 1006 ppm of Sn. According to Kowalski et al. [25], it is assumed that Sn atoms in PLLA-ap are bonding through alkoxide groups to polymer chain ends to form “PLLA-O-Sn”. After the polymerization, PLLA-ap was dissolved in chloroform and precipitated with excess methanol to prepare precipitated PLLA (PLLA-pr) containing 689 ppm of Sn. During the precipitation process, the end structure of “PLLA-O-Sn” will exchange with

methanol to form “PLLA-OH” [26]. According to the previous reports [27-29], Sn atoms in PLLA are not removable by the dissolution/precipitation method. It is considered that after the precipitation process the Sn atoms in PLLA-pr are bonding to polymer chain ends in the form of a salt, “HO-PLLA-COO^- $Sn^{2+}X^-$“. To prepare a metal free polymer, PLLA-pr was purified by a liquid-liquid extraction method with 1**M** HCl [14,23,29,30], resulting in the formation of purified PLLA-H containing 23 ppm of Sn, which was close to the lower limits of detection.

The three PLLA-samples have different Sn contents and nearly equal molecular weights (Table 1). This allows us to evaluate the effect of the end-structure on the thermal degradation of PLLA without any consideration needing to be given to the influence of the molecular weight of the samples.

3.2. Dynamic pyrolysis of PLLA-ap, PLLA-pr, and PLLA-H

Thermogravimetric analysis (TG) is a commonly employed approach for evaluating the thermal properties of polymer materials. To analyze the thermal degradation behavior of PLLA samples with different end structures, the dynamic thermal degradation of film samples was conducted with TG/DTA by measuring the weight loss as a function of linear increase in temperature in a nitrogen atmosphere. The TG measurement was carried out at various heating rates (ϕ) of 1~9 K min^{-1}. Typical weight loss profiles for PLLA-ap, PLLA-pr, and PLLA-H at ϕ = 5 K min^{-1} are shown in Figure 1.

[**Figure 1**. TG profiles (5 K min^{-1})]

Each sample showed individual TG curves in a different temperature range. The weight loss of

PLLA-ap started at about 150 °C (1 K min^{-1}) and finished at about 290 °C (9 K min^{-1}). An obvious increase in degradation temperature was shown in the TG curve of PLLA-pr. The weight loss of PLLA-pr started at about 230 °C (1 K min^{-1}) and proceeded rapidly to complete degradation at about 320 °C (9 K min^{-1}) within a narrow temperature range. PLLA-H degraded at the highest temperature, starting at about 250 (1 K min^{-1}) and finishing at about 385 °C (9 K min^{-1}). The individual profiles of each TG curve are best explained by assuming that a different degradation reaction occurred in each temperature range, rather than being due to a simple lowering of the degradation temperature as a result of the increase in Sn content.

3.3. Pyrolyzates

Here, the effects of the end-structure were also examined by analysis of pyrolyzates evolved from PLLA-samples. Figure 2 shows Py-GC/MS chromatograms of pyrolyzates of PLLA-ap, PLLA-pr, and PLLA-H evolved in temperature ranges of 60-280, 60-380, and 60-400 °C, respectively, at a heating rate of 10 °C min^{-1}. All samples showed a main peak at 13.4-13.7 min in retention time. This peak has been confirmed to be L,L-/D,D-lactide by comparing it with that of the standard substance [23,31]. Evolution of *meso*-lactide was determined by a peak at 12.2 min in the chromatogram of PLLA-H, but this peak was hardly visible in the chromatograms of PLLA-ap and PLLA-pr. These chromatograms suggest that both pyrolysis of PLLA-ap and PLLA-pr resulted in a selective L,L-lactide production. In contrast, the chromatogram of PLLA-H shows a large amount of meso-lactide and other cyclic oligomers. A series of

peaks periodically appearing in groups at 23-33 min represents the production of cyclic oligomers from trimer to octamer, which are made up of each group of diastereoisomers [14,23,30,32,33].

[**Figure 2**. Py-GC/MS chromatograms]

To determine the changes in the composition of pyrolyzates from PLLA samples, the pyrolyzates evolved in different temperature ranges were collected and analyzed with Py-GC/MS. Results of the composition analysis are illustrated in Figure 3, in which each component content was calculated from the peak intensity in Py-GC/MS chromatogram. The pyrolyzates from PLLA-ap were almost all L,L-lactide with a little *meso*-lactide (<1.3 %) over the whole degradation range (180-300 °C). In addition to the dominant L,L-lactide, the pyrolyzates from PLLA-pr were also composed of a small amount of *meso*-lactide (<1.9 %), despite the higher degradation temperature range of 260-340 °C. Witzke et al. reported the formation of 2 % *meso*-lactide at a conversion greater than 90 % on $Sn(Oct)_2$-catalyzed polymerization of L,L-lactide at 130 °C [13]. Therefore, a small amount of *meso*-lactide in PLLA-ap and PLLA-pr pyrolyzates may be formed before the pyrolysis. On the other hand, the pyrolyzates evolved from PLLA-H were composed of L,L-/D,D-lactides (83-27 %) and a large amount of *meso*-lactide (8-15 %) and cyclic oligomers (total 3-64 %) in a temperature range of 300-400 °C. The production of cyclic oligomers was enhanced significantly with increase in temperature.

These results clearly indicate that the residual Sn compounds markedly influence the pyrolysis of PLLA, and that each PLLA sample with a different end structure degrades through a different reaction.

[**Figure 3**. Composition of pyrolyzates]

3.4. Apparent activation energy of thermal degradation

Influences of PLLA-Sn end structures on the thermal degradation kinetics were analyzed from TG data of PLLA samples conducted at various heating rates of 1, 3, 5, 7, and 9 K min^{-1}. The apparent activation energy, E_a, of the thermal degradation was estimated from the weight loss data according to a previously published method [34-37]. Figure 4a shows changes in the E_a values during the pyrolysis of PLLA-ap, PLLA-pr, and PLLA-H with changes in the fractional weight, *w*. Each sample exhibits a characteristic E_a curve. The E_a value of PLLA-ap decreased gradually from 99 to 82 kJ mol^{-1} with increase in weight loss. This change in E_a value closely follows the first half of the change reported by Babanalbandi et al. [15]. In the case of PLLA-pr, the E_a value was relatively constant at 127-133 kJ mol^{-1} during the whole pyrolysis. This result is comparable with E_a = 120-130 kJ mol^{-1} of precipitated PLLA samples containing 169-607 ppm of Sn in the previous report [23]. Thus, the E_a value of about 120-130 kJ mol^{-1} must be a fixed parameter for a typical pyrolysis mechanism caused by a PLLA-Sn end structure. Obviously, the gap in E_a value between PLLA-ap and PLLA-pr pyrolysis is significant, reflecting differences in the pyrolysis mechanism, but cannot simply be explained as being due only to a difference in the Sn content. The E_a value of PLLA-H, which started from about 135 kJ mol^{-1} and rose to 176 kJ mol^{-1} as degradation progressed, agrees with the previously reported values for purified PLLA [23,30]. These results indicate that the PLLA-Sn end structure is a principal factor in the PLLA pyrolysis.

[**Figure 4**. Changes in E_a value]

In Figure 4b, the E_a values were plotted against temperature. Each E_a curve occupies an isolated position in temperature scale without any overlap. This suggests that one kind of end-structure causes a characteristic degradation reaction in a particular temperature range. The previously reported complicated E_a changes in PLLA pyrolysis on a heating process must have reflected the stepwise changes in these plural reactions during the degradation process [15,16].

The characteristic degradation reaction in each particular temperature range was analyzed by kinetics approaches in the next section.

3.5. Kinetics of PLLA-ap, PLLA-pr, and PLLA-H pyrolysis

The thermal degradation kinetics of the PLLA samples was studied by several analytical approaches [36,38-40]. The integration analysis plots for the experimental data of PLLA-ap (9 K min^{-1}) and the model reactions are illustrated in Figure 5. In this Figure, $\theta = (E_a/\phi R)p(y)$ is defined as the reduced time, where R is the molar gas constant and function $p(y)$ is tabulated by Doyle [36,41]. It was observed that the degradation of PLLA-ap closely followed the zero-order reaction simulation with parameter values: E_a = 85 kJ mol^{-1} and pre-exponential value $A = 6.8 \times 10^5$ s^{-1}. Interestingly, the main part of the experimental plot could also be closely matched by superimposing the random degradation simulation (L=3) with parameter values: E_a = 85 kJ mol^{-1} and $A = 1.0 \times 10^6$ s^{-1}, where L is the least number of repeating units of oligomer not volatilized (data not shown). In both mechanisms, L,L-lactide is produced dominantly. Considering the gradual E_a change, it is assumed that similar plural reactions are occurring during the pyrolysis with their

proportional contributions changing with temperature. Thus, it is considered that a minor random degradation process occurs at the same time as an *n*th-order degradation process and contributes to the resulting zero-order weight loss behavior. In the final stage of the pyrolysis, the experimental plot deviated from the simulation plots due to the influence of end residues.

[**Figure 5**. PLLA-ap: Integration analyses]

In Figure 6, the experimental data of PLLA-pr (1 K min^{-1}) and model reactions with E_a = 130 kJ mol^{-1} and $A = 6.2 \times 10^9$ s^{-1} were plotted by the integral method. This data plot clearly shows both weight loss behaviors in the initial and main periods. After the slow weight loss in the initial period, the experimental plot showed a linear relationship between w and A, in parallel to the zero-order reaction simulation plot. Nearly the same result was found in the pyrolysis of precipitated PLLA containing 607 ppm of Sn in the previous report [23]. Thus, it is clear that the main degradation process of PLLA-pr is a zero-order weight loss process, and the slow weight loss process in the initial period could be regarded as a random decomposition process simulated, apparently, with E_a = 130 kJ mol^{-1} and $A = 1.0 \times 10^9$ s^{-1}. Though both main degradation processes of PLLA-ap and PLLA-pr are regarded as being the zero-order weight loss process, each elementary reaction will be different because of the significant gaps in the kinetic parameters.

[**Figure 6**. PLLA-pr: Integration analysis]

In Figure 7, the random degradation analysis plots of $\log[-\log\{1-(1-w)^{0.5}\}]$ vs $1/T$ for experimental data of PLLA-H (9 K min^{-1}) and model reactions are illustrated with kinetic parameters: E_a = 175 kJ mol^{-1}

and $A = 1.25 \times 10^{12}$ s^{-1}. Obviously, the experimental data plot closely followed the *n*th-order reaction plots at the first stage, but then shifted onto a random degradation plot with *L*=4-5 in the following stage. This simulation of PLLA-H pyrolysis is nearly the same as that for the purified PLLA pyrolysis reported previously [23,30]. The simulated random degradation, *L*=4-5 supports the evidence of the production of the cyclic oligomers found in Figures 2 and 3.

[**Figure 7**. PLLA-H: Random degradation analysis]

Therefore, the thermal degradation of each PLLA sample proceeds through characteristic plural reactions with each reaction having peculiar kinetic parameters. The estimated kinetic parameters, E_a, *A*, and the reaction order are listed in Table. 2. These results settle the previous discussion, as to whether the PLLA thermal degradation is a random or *n*th-order degradation process.

[**Table 2**. Kinetic parameters]

3.6. Mechanisms of PLLA-ap, PLLA-pr, and PLLA-H pyrolysis

The Sn-catalyzed polymerization of L,L-lactide is a typical equilibrium polymerization [12,13]. It is considered that the thermal degradation of PLLA-ap proceeds in a similar way to the depolymerization mechanism in the equilibrium polymerization of L,L-lactide [26]. Thus, the active end structure will be Sn-alkoxide, and the alkoxide anion attacks an electron-poor carbonyl carbon in lactate unit, which coordinates on an Sn atom, resulting in the polymerization or depolymerization [9,24,25]. The nucleophilic attack can occur at intra- and inter-molecular level, namely, the backbiting and bimolecular

transesterification reactions. In particular, the repeating backbiting reactions onto carbonyl carbon in the penultimate unit result in unzipping depolymerization, which produces lactide selectively. As reported previously [23], it should be noted that the unzipping depolymerization of polymer with polydispersity index ~2 shows a 1st-order weight loss behavior. To show the zero-order weight loss behavior along with the unzipping depolymerization, a cooperative random bimolecular transesterification is indispensable. In this process, the polymer can be regarded as being a monodisperse polymer during the depolymerization process. Kowalski et al. estimated that the ratio of the rate constant for the polymerization, k_p, and bimolecular transesterification, k_{tr2}, on solution polymerization of L,L-lactide was 200 at 80 °C [26]. Bimolecular transesterification must also occur in the thermal degradation. The observed zero-order weight loss behavior will be the result of a combination of main unzipping depolymerization and minor bimolecular transesterification reactions caused by alkoxide anions at chain ends (Scheme 1). Oligomer formation is expected via the transesterification reaction, however, these oligomers are not easily volatilized at temperatures less than 270 °C and undergo further reaction before finally changing into volatile lactides.

[**Scheme 1**. PLLA-ap pyrolysis mechanism]

Kinetic and pyrolyzates analyses show the pyrolysis of PLLA-pr will proceed mainly through the zero-order weight loss process to produce selectively L,L-lactide. Interestingly, no cyclic oligomer was detected during the pyrolysis, despite the temperatures being high enough (300-340 °C) to cause cyclic oligomers to volatilize, as shown in PLLA-H pyrolysis (Figure 3). These results support the Sn-catalyzed

selective lactide elimination mechanism by carboxylate-Sn species at chain ends (Scheme 2), which was the mechanism proposed previously for precipitated PLLA pyrolysis [23]. Though this reaction is first-order in active Sn atoms, it leads to the zero-order with respect to *w* of PLLA-pr.

[**Scheme 2**. PLLA-pr pyrolysis mechanism]

The pyrolysis of PLLA-H has been reported to proceed mainly through the random degradation (L = 4) from the kinetic analysis of TG/DTA data [23,30]. In this study, nearly the same kinetics: random degradation (L=4-5) was estimated. Particularly, the large amount of *meso*-lactide and cyclic oligomers produced means that racemization occurs easily during the pyrolysis of PLLA-H, whereas little racemization occurs during PLLA-ap and PLLA-pr pyrolysis. This production of cyclic oligomers and diastereoisomers will be due to the random reactions caused by hydroxyl and carboxyl end groups and the ester-semiacetal tautomerization occurring at temperatures above 300 °C (Scheme 3) [14,30,31].

These proposed degradation mechanisms for the PLLA samples clarify the significance of the effect of PLLA-Sn end structures, making it clear that the proposed mechanisms contribute to the interpretation of the previously reported complicated PLLA pyrolysis behavior.

[**Scheme 3**. PLLA-H pyrolysis mechanism]

4. Conclusion

To clarify the pyrolysis mechanism of PLLA containing Sn atoms, three samples with different chain end structures, namely, as-polymerized PLLA-ap, precipitated-with-methanol PLLA-pr, and purified

PLLA-H, were prepared. From the pyrolyzate analysis with Py-GC/MS and the kinetic analysis of thermogravimetric data of the samples, typical degradation mechanisms for the Sn-containing PLLAs were proposed. That is, it is assumed that the pyrolysis of PLLA-ap proceeds through a zero-order weight loss process with apparent E_a = 80-90 kJ mol^{-1} at the lowest temperatures, with the process being composed of the backbiting and transesterification reactions caused by Sn-alkoxide chain ends. The pyrolysis of PLLA-pr was also assumed to proceed via a zero-order weight loss process with apparent E_a =120-130 kJ mol^{-1}. This reaction was proposed as being the Sn-catalyzed selective lactide elimination caused by Sn-carboxylate chain ends. Both the pyrolysis of PLLA-ap and PLLA-pr produced L,L-lactide selectively. These degradation mechanisms and pyrolyzates are in contrast to those of PLLA-H, which showed random degradation, with apparent E_a = 176 kJ mol^{-1} at highest temperatures, to form a large amount of diastereoisomers and cyclic oligomers. From this study, the complicated PLLA pyrolysis process could be explained properly.

References

[1] Ikada Y, Tsuji H. Biodegradable polyesters for medical and ecological applications. Macromol Rapid Commun 2000; 21(3): 117-32.

[2] Amass W, Amass A, Tighe B. A review of biodegradable polymers: Uses, current developments in the synthesis and characterization of biodegradable polyesters, blends of biodegradable polymers and recent advances in biodegradation studies. Polym Int 1998;47(2):89-144.

[3] Anderson JM, Shive MS. Biodegradation and biocompatibility of PLA and PLGA microspheres. Advan Drug Delivery Rev 1997;28(1):5-24.

[4] Ajioka M, Enomoto K, Suzuki K, Yamaguchi A. The basic properties of poly (lactic acid) produced

by the direct condensation polymerization of lactic acid. J Environ Polym Degrad 1995;3(4):225-34.

[5] Urayama H, Ohara H. Crystallinity and molding properties of polylactic acid (Lacty®). Shimadzu Hyoron 2000;56:163-8.

[6] Tuominen J, Kylma J, Kapanen A, Venelampi O, Itavaara M, Seppala J. Biodegradation of lactic acid based polymers under controlled composting conditions and evaluation of the ecotoxicological impact. Biomacromolecules 2002;3:445-55.

[7] Lunt J. Large-scale production, properties and commercial applications of polylactic acid polymers. Polym Degrad Stab 1998;59:145-52.

[8] Leenslag JW, Pennings AJ. Synthesis of high-molecular-weight poly(L-lactide) initiated with tin 2-ethylhexanoate. Makromol Chem 1987;188:1809-14.

[9] Kricheldorf HR, Kreiser-Saunders I, Stricker A. Polylactones 48. $SnOct_2$-initiated polymerization of lactide: a mechanistic study. Macromolecules 2000;33:702-9.

[10] Kowalski A, Duda A, Penczek S. Polymerization of L,L-lactide initiated aluminum isopropoxide trimer or tetramer. Macromolecules 1998;31:2114-22.

[11] Nomura N, Ishii R, Akakura M, Aoi K. Stereoselective ring-opening polymerization of racemic lactide using aluminum-achiral ligand complexes: Exploration of a chain-end control mechanism. J Am Chem Soc 2002;124:5938-9.

[12] Duda A, Penczek S. Thermodynamics of L-lactide polymerization. Equilibrium monomer concentration. Macromolecules 1991;23:1636-9.

[13] Witzke DR, Narayan R, Kolstad JJ. Reversible kinetics and thermodynamics of the homopolymerization of L-lactide with 2-ethylhexanoic acid tin(II) salt. Macromolecules 1997;30:7075-85.

[14] Kopinke FD, Remmler M, Mackenzie K, Moder M, Wachsen O. Thermal decomposition of biodegradable polyesters-II. Poly (lactic acid). Polym Degrad Stab 1996;53;329-42.

[15] Babanalbandi A, Hill DJT, Hunter DS, Kettle L. Thermal stability of poly (lactic acid) before and after ^{3}-radiolysis. Polym Int 1999;48:980-4.

[16] Aoyagi Y, Yamashita K, Doi Y. Thermal degradation of poly[(R)-3-hydroxybutyrate], poly [μ-caprolactone], and poly[(S)-lactide]. Polym Degrad Stab 2002;76:53-9.

[17] Ajioka M, Enomoto K, Suzuki K, Yamaguchi A. Basic properties of polylactic acid produced by the

direct condensation polymerization of lactic acid. Bull Chem Soc Jpn 1995;68:2125-31.

[18] Tsuji H, Ikada Y. Stereocomplex formation between enantiomeric poly(lactic acid)s. 6. Binary blends from copolymers. Macromolecules 1992; 25: 5719-23.

[19] Radano CP, Baker GL, Smith MR. Stereoselective polymerization of a racemic monomer with a racemic catalyst: direct preparation of the polylactic acid stereocomplex from racemic lactide. J Am Chem Soc 2000;122:1552-3.

[20] Food Drug Adm. Food additives. Resinous and polymeric coatings. Fed Regist 1975;40(121) C (23. Jun 1975) (CA 83: 112493h).

[21] Södergård A, Näsman JH. Melt stability study of various types of poly(L-lactide). Ind Eng Chem Res 1996;35:732-5.

[22] Wachsen O, Platkowski K, Reichert KH. Thermal degradation of poly-L-lactide – studies on kinetics, modeling and melt stabilization. Polym Degrad Stab 1997;57:87-94.

[23] Nishida H, Mori T, Hoshihara S, Fan Y, Shirai Y, Endo T. Effect of tin on poly(L-lactic acid) pyrolysis. Polym Degrad Stab 2003;81:515-23.

[24] Kricheldorf HR, Kreiser-Saunders I, Boettcher C. Polylactones: 31. Sn(II) octoate-initiated polymerization of L-lactide: a mechanistic study. Polymer 1995;36:1253-9.

[25] Kowalski A, Duda A, Penczek S. Kinetics and mechanism of cyclic esters polymerization initiated with tin(II) octoate. 3. Polymerization of L,L-dilactide. Macromolecules 2000;33:7359-70.

[26] Kowalski A, Libiszowski J, Duda A, Penczek S. Polymerization of L,L-dilactide initiated by tin(II) butoxide. Macromolecules 2000;33:1964-71.

[27] Zhang X, Wyss UP, Pichora D, Goosen MFA. An investigation of the synthesis and thermal stability of poly(DL-lactide). Polym Bull 1992;27:623-9.

[28] Schwach G, Coudane J, Engel R, Vert M. Zn lactate as initiator of DL-lactide ring opening polymerization and comparison with Sn octoate. Polym Bull 1996;37:771-6.

[29] Cam D, Marucci M. Influence of residual monomers and metals on poly(L-lactide) thermal stability. Polymer 1997;38:1879-84.

[30] Fan Y, Nishida H, Hoshihara S, Shirai Y, Tokiwa Y, Endo T. Pyrolysis Kinetics of Poly(L-lactide) with Carboxyl and Calcium Salt End Structures. Polym Degrad Stab 2003;79:547-62.

[31] Fan Y, Nishida H, Shirai Y, Endo T. Racemization on thermal degradation of poly(L-lactide) with

calcium salt end structure. Polym Degrad Stab 2003;80:503-11.

[32] Khabbaz F, Karlsson S, Albertsson AC. Py-GC/MS an effective technique to characterizing of degradation mechanism of poly (L-lactide) in the different environment. J Appl Polym Sci 2000;78:2369-78.

[33] Westphal C, Perrot C, Karlsson S. Py-GC/MS as a means to predict degree of degradation by giving microstructural changes modeled on LDPE and PLA. Polym Degrad Stab 2001;73:281-7.

[34] Doyle CD. Estimating isothermal life from thermogravimetric data. J Appl Polym Sci 1962;6:639-42.

[35] Reich L. A rapid estimation of activation energy from thermogravimetric traces. Polym Lett 1964;2:621-3.

[36] Ozawa T. A new method of analyzing thermogravimetric data. Bull Chem Soc Japan 1965;38:1881-6.

[37] Nishida H, Yamashita M, Hattori N, Endo T, Tokiwa Y. Thermal decomposition of poly(1,4-dioxan-2-one). Polym Degrad Stab 2000;70:485-96.

[38] Flynn JH, Wall LA. General treatment of the thermogravimetry of polymers. J Res Nat Bur Stand 1966;70A:487-523.

[39] Ichihara S, Nakagawa H, Tsukazawa Y. Thermal decomposition behaviors of polymers analyzed with thermogravimetry. Kobunshi Ronbunshu 1994;51(7):459-65.

[40] Nishida H, Yamashita M, Endo T. Analysis of initial process in pyrolysis of poly (*p*-dioxanone). Polym Degrad Stab 2002;78:129-35.

[41] Doyle CD, Kinetic analysis of thermogravimetric data. J Appl Polym Sci 1961;5:285-92.

Table 1. PLLA samples

Sample	Description	M_n	M_w	Sn content (ppm)
PLLA-ap	As-polymerized	223,000	451,000	1,006
PLLA-pr	Precipitated with methanol	217,000	429,000	689
PLLA-H	Extracted with 1**M** HCl aq.	266,000	494,000	23

Table 2. Kinetic parameters for PLLA-ap, PLLA-pr, and PLLA-H pyrolysis

Sample	Initial stage (w >0.9)			Main stage		
	E_a (kJ mol^{-1})	A (s^{-1})	n / random: L	E_a (kJ mol^{-1})	A (s^{-1})	n / random: L
PLLA-ap	95	1.2 x 10^{7}	nth + random	85	6.8 x 10^{5} (1.0 x 10^{6})	n = 0 (random, L=3)
PLLA-pr	130	1.0 x 10^{9}	random, L=3	130	6.2 x 10^{9}	n = 0
PLLA-H	135	3.5 x 10^{8}	nth + random	175	1.25 x 10^{12}	random, L=4-5

Figure Legend

Figure 1. Thermogravimetric curves of PLLA-ap, PLLA-pr, and PLLA-H decomposition at a heating rate of 5 K min^{-1} under N_2 flow of 100 ml min^{-1}.

Figure 2. Py-GC/MS (TIC) chromatograms of PLLA-ap, PLLA-pr, and PLLA-H pyrolyzates in different heating processes of 60-280 ˚C (PLLA-ap), 60-380 ˚C (PLLA-pr), and 60-400 ˚C (PLLA-ap), respectively, at a constant heating rate of 10 ˚C min^{-1}.

Figure 3. Volatile products on PLLA sample pyrolysis in different temperature ranges. Content ratio (%) of meso-, D,D- or L.L-lactide, and higher cyclic oligomers including trimers to octamers.

Figure 4. Apparent activation energies of PLLA-ap, PLLA-pr, and PLLA-H

Figure 5. Plots of experimental $(AE_a/\phi R)p(y)$ $(=A\theta)$ vs w of PLLA-ap at a heating rate of 9 K min^{-1} (E_a = 85 kJ mol^{-1} and $A = 6.8 \times 10^5$ s^{-1}), and for model reactions. Model reactions: zero- (n = 0), half- (n=0.5), 1st- (n = 1), and 2nd-order (n = 2), and random degradations (random L = 2-3).

Figure 6. Plots of experimental ($AE_a/\phi R)p(y)$ ($=A\theta$) vs w of PLLA-pr at a heating rate of 1 K min^{-1} (E_a = 130 kJ mol^{-1} and A = 6.2 × 10^9 s^{-1}), and for model reactions. Model reactions: zero- (n = 0), half- (n=0.5), 1st- (n = 1), and 2nd-order (n = 2), and random degradations (random L = 2-4).

Figure 7. Plots of log[-log{1-(1-w)$^{1/2}$}] vs. 1/T for thermogravimetric data of PLLA-H at a heating rate of 9 K min^{-1} (E_a = 175 kJ mol^{-1} and A = 1.25 × 10^{12} s^{-1}), and for model reactions. Model reactions: zero- (n = 0), half- (n=0.5), 1st- (n = 1), and 2nd-order (n = 2), and random degradations (random L = 2-5).

Scheme 1. Possible unzipping and transesterification reactions on PLLA-ap decomposition

Scheme 2. Possible selective lactide elimination on PLLA-pr decomposition

Scheme 3. Possible random degradation reactions on PLLA-H decomposition

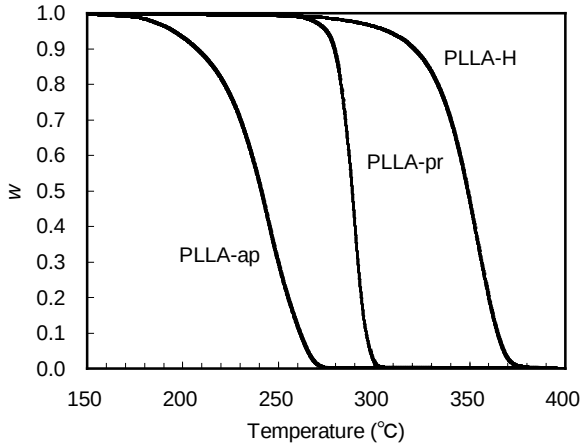

Figure 1.

Mori & Nishida

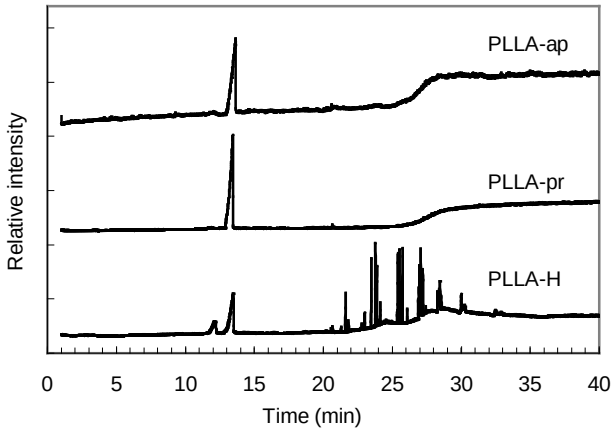

Figure 2.

Mori & Nishida

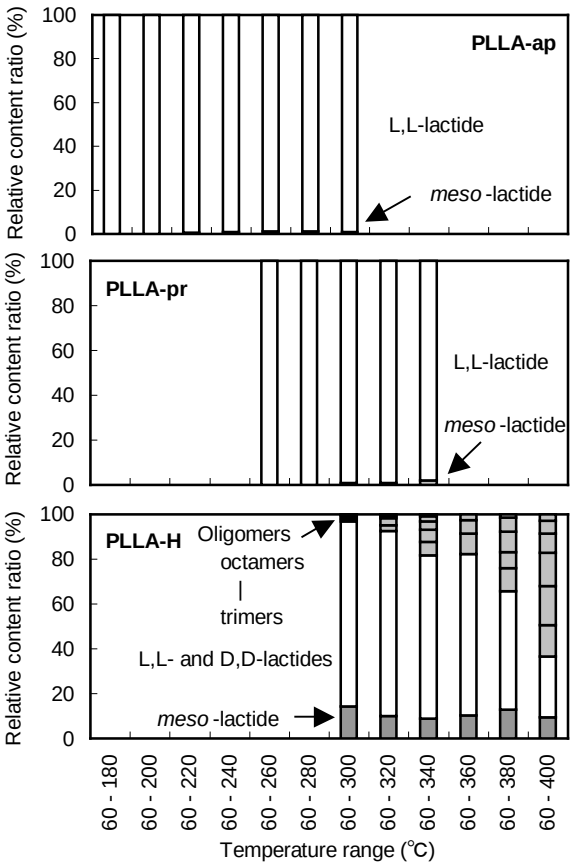

Figure 3.

Mori & Nishida

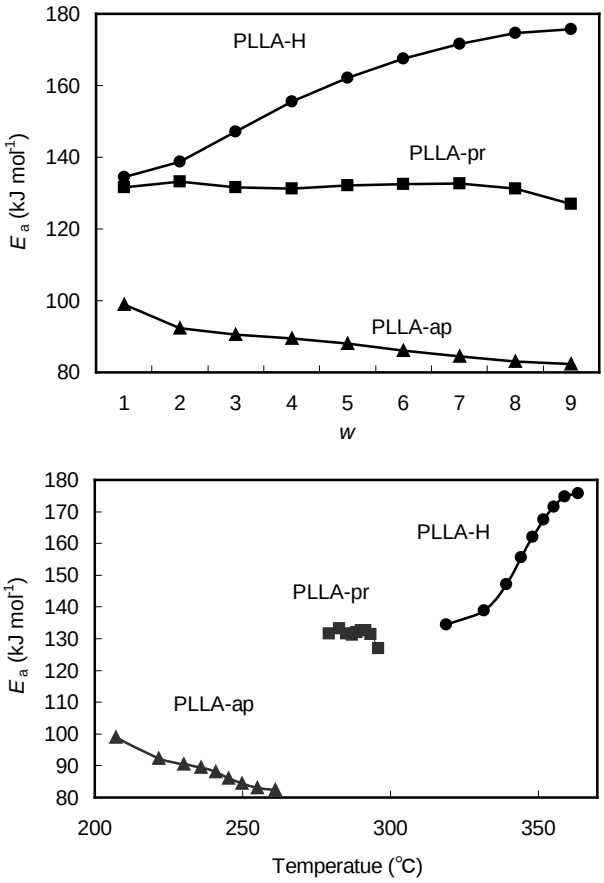

Figure 4.

Mori & Nishdia

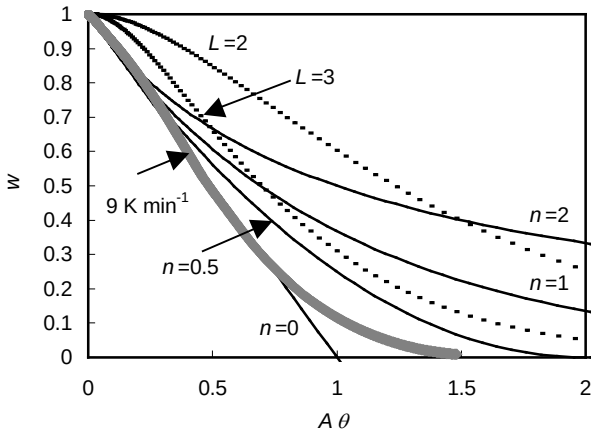

Figure 5.

Mori & Nishida

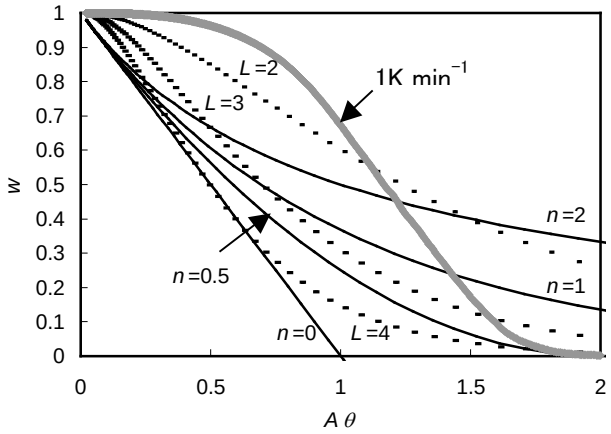

Figure 6.

Mori & Nishida

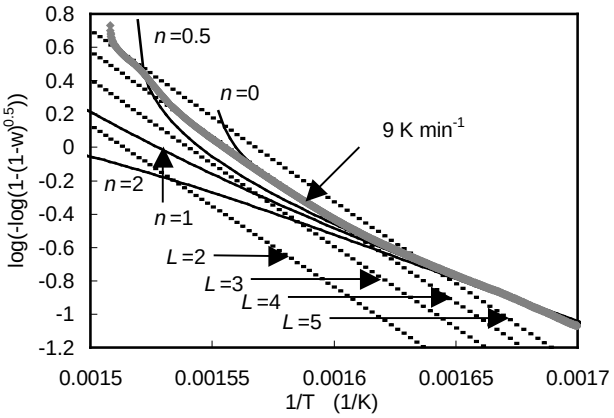

Figure 7.

Mori & Nishida

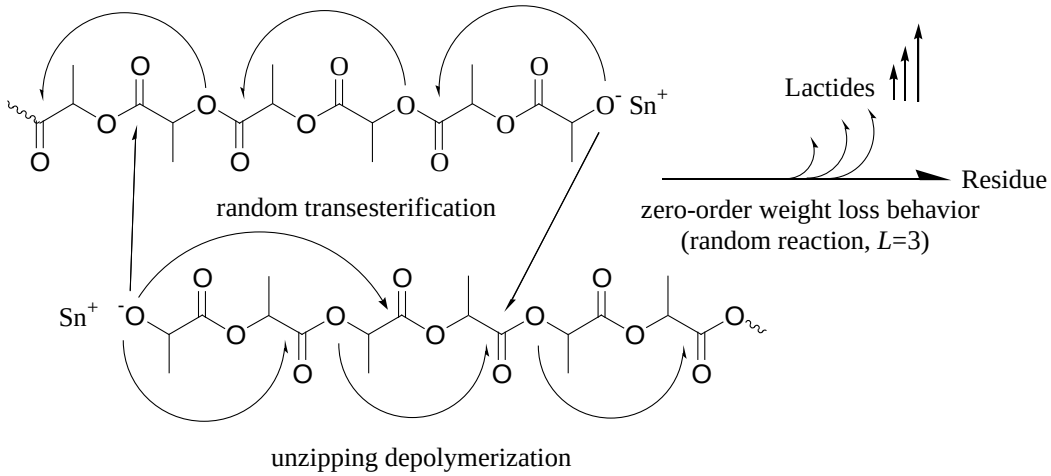

Scheme 1

Mori & Nishdia

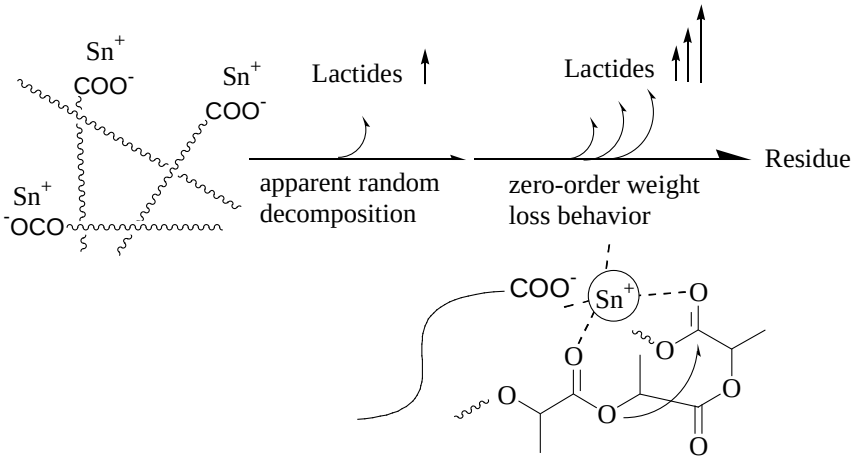

Scheme 2.

Mori & Nishida

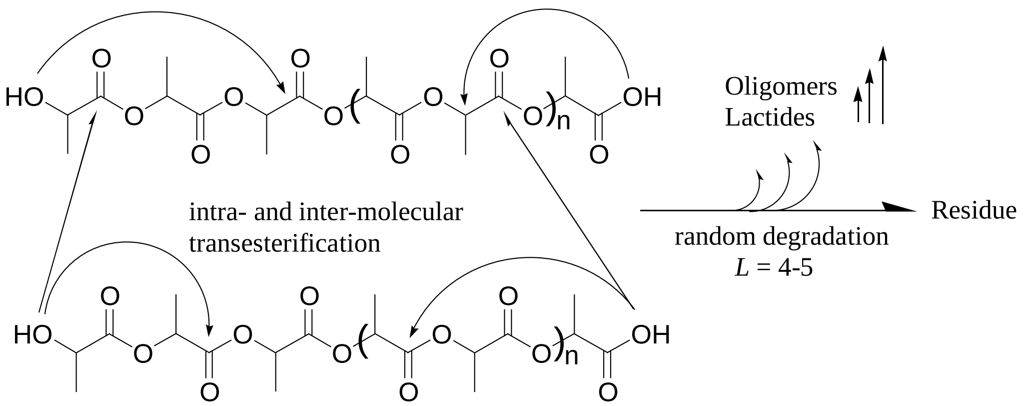

Scheme 3

Mori & Nishida